Path-Following Control of Autonomous Underwater Vehicles Subject to Velocity and Input Constraints via Neurodynamic Optimization

Zhouhua Peng, *Member, IEEE*, Jun Wang, *Fellow, IEEE*, and Qing-Long Han, *Fellow, IEEE*

***Abstract*—In this paper, a design method is presented for path-following control of underactuated autonomous underwater vehicles subject to velocity and input constraints, as well as internal and external disturbances. In the guidance loop, a kinematic control law of the desired surge speed and pitch rate is derived based on a backstepping technique and a line-of-sight guidance principle. In the control loop, an extended state observer is developed to estimate the extended state composed of unknown internal dynamics and external disturbances. Then, a disturbance rejection control law is constructed using the extended state observer. To bridge the guidance loop and the control loop, a reference governor is proposed for computing optimal guidance signals within the velocity and input constraints. The reference governor is formulated as a quadratically constrained optimization problem. A projection neural network is employed for solving the optimization problem in real time. Simulation results illustrate the effectiveness of the proposed method for path-following control of autonomous underwater vehicles subject to constraints and disturbances simultaneously in the vertical plane.**

***Index Terms*—Autonomous underwater vehicles (AUVs), extended state observer (ESO), input and state constraints, neurodynamic optimization, path following.**

Manuscript received June 30, 2018; revised September 24, 2018 and October 26, 2018; accepted November 23, 2018. Date of publication December 13, 2018; date of current version June 28, 2019. This work was supported in part by the Research Grants Council of the Hong Kong Special Administrative Region, China, under Grant 14207614 and Grant 11208517, in part by the Australian Research Council Discovery Project under Grant DP160103567, in part by the National Natural Science Foundation of China under Grant 51579023, Grant 61673330, and Grant 61673081, in part by the Innovative Talents in Universities of Liaoning Province under Grant LR2017014, in part by High Level Talent Innovation and Entrepreneurship Program of Dalian under Grant 2016RQ036, and in part by the Fundamental Research Funds for the Central Universities under Grant 3132016313 and Grant 3132018306. *(Corresponding author: Jun Wang.)*

Z. Peng is with the School of Marine Electrical Engineering, Dalian Maritime University, Dalian 116026, China, and also with the Department of Computer Science, City University of Hong Kong, Kowloon, Hong Kong (e-mail: zhpeng@dlmu.edu.cn).

J. Wang is with the Department of Computer Science, City University of Hong Kong, Kowloon, Hong Kong, and also with the City University of Hong Kong–Shenzhen Research Institute, Shenzhen 518172, China (e-mail: jwang.cs@cityu.edu.hk).

Q.-L. Han is with the School of Software and Electrical Engineering, and Swinburne University of Technology, Melbourne, VIC 3122, Australia (e-mail: qhan@swin.edu.au).

Color versions of one or more of the figures in this paper are available online at http://ieeexplore.ieee.org.

Digital Object Identifier 10.1109/TIE.2018.2885726

I. Introduction

AUTONOMOUS marine vehicles, including surface and underwater vehicles, are characterized by small size, low cost, autonomy, and intelligence. They are widely developed and deployed to conduct various missions such as ocean sampling, resource exploration and exploitation, and sensor networks, with minimal or without human supervision [1]–[10]. During the past few years, many results on motion control of marine vehicles are reported [11]–[22]. Several motion control scenarios are targeted, such as trajectory/target tracking [18]–[20], [23], [24], formation producing/tracking [25], [26], and path following [1]–[4], [12]–[14], [16], [17], [27], [28]. In particular, the path-following problem has drawn compelling interest, and a number of methods have been proposed with different focuses. In [2], a backstepping design technique is employed to develop a nonlinear feedback controller for path following of an underactuated autonomous underwater vehicle (AUV). In [3], a hybrid adaptation scheme is introduced to enhance the robustness against the parametric uncertainty. In [4], an adaptive switching control law is developed for path following of autonomous vehicles moving in a three-dimensional (3-D) space. Due to its simplicity and function to mimic a practiced helmsman [12], a line-of-sight (LOS) guidance scheme is widely incorporated into the path-following design for achieving the convergence to a desired path [13], [14], [16], [17], [27], [28]. In [13], a κ-exponentially stable integral LOS guidance law is presented for straight-line path following that is capable of eliminating the effect of constant external disturbances. In [14], an adaptive integral LOS guidance law for path following is proposed. In [17], a nonlinear LOS path-following controller is presented for AUVs, enabling smooth transitions between fully actuated and underactuated configurations. In [16], a 3-D integral LOS guidance and control method is proposed for straight-line path following of AUVs. In [27], a predictor-based LOS guidance law is developed for path following of surface vehicles with fast sideslip compensation. In [28], an extended-state-observer (ESO)-based LOS guidance law for path following of

underactuated surface vehicles is presented, enabling the exact estimation of the sideslip angle. However, the physical constraints are not addressed in [1]–[4], [12]–[14], [16], [17], and [27]–[29].

Constraints are ubiquitous and naturally arise in control systems [8], [30]–[38]. Violating system constraints may degrade control performance and result in a failure of control in the worst case. Some attempts have been made to address the constraint problem in motion control of marine vehicles [8], [39]–[45]. In [8], [41], and [44], an auxiliary system design is used to pull out the control signal from saturation. When the state and input are concerned, most works are practiced within the model-predictive control (MPC) framework. In [40], an MPC scheme is employed for LOS path following of underactuated surface vessels. In [39], an MPC law is proposed for trajectory tracking of underactuated vessels. In [42], a trajectory tracking controller for surface craft is developed based on a nonlinear MPC scheme. In [45], an MPC approach is proposed for stabilization of underactuated AUVs. In general, the MPC methods require that the vehicle models are accurately known for prediction. However, the accurate model may not be obtained in practice. Moreover, a well-established AUV model may suffer from parametric perturbations, external disturbances, and modeling errors. Therefore, it is of great significance to address the path-following control of AUVs in the presence of unknown kinetics and physical constraints simultaneously.

In this paper, a method is presented for path-following control of an underactuated AUV subject to velocity and input constraints, as well as internal model uncertainty and external environmental forces. A virtual guidance law of surge speed and pitch rate is first designed to stabilize the along-track error and the cross-track error in the guidance loop. In the control loop, an ESO is developed to estimate the model uncertainty and external disturbance. Then, an ESO-based disturbance rejection control law is constructed at the kinetic level. By taking the velocity and input constraints into account, a reference governor is used for computing optimal guidance signals by balancing the virtual guidance signal and the current velocity signal of the AUV. The reference governor is formulated as a quadratically constrained optimization problem, and a projection neural network is employed for solving the optimization problem in real time. The stability of the closed-loop path-following system is analyzed based on cascade system stability. Simulation results substantiate the efficacy of the proposed neurodynamic optimization approach to path-following control of underactuated AUVs subject to velocity and input constraints, as well as internal and external disturbances. The proposed method can be used in various missions such as bottom-following or seabed tracking tasks [46], [47].

Compared with some existing results, the salient features of the proposed method are as follows. In contrast to the path-following controllers proposed in [2], [3], [12]–[14], [16], [17], [27], and [28], where the physical constraints are not considered, the presented work addresses the path-following control problem in the case of the unknown disturbances and physical constraints, simultaneously. Compared with the MPC methods in [34], [39], [40], [42], and [45], where the AUV models should be exactly known, the proposed optimization-based reference governor takes the constraint-handling capability without requiring the accurate model of the AUV. Due to the lack of an exact AUV model for prediction, the MPC methods given in [34], [39], [40], [42], and [45] are not applicable. Besides, the vehicle kinetics can be totally unknown and is accurately estimated by the ESO. The auxiliary system design in [8], [41], and [44] is only able to address the input constraint, while the proposed neurodynamic optimization approach allows one to handle state and input constraints.

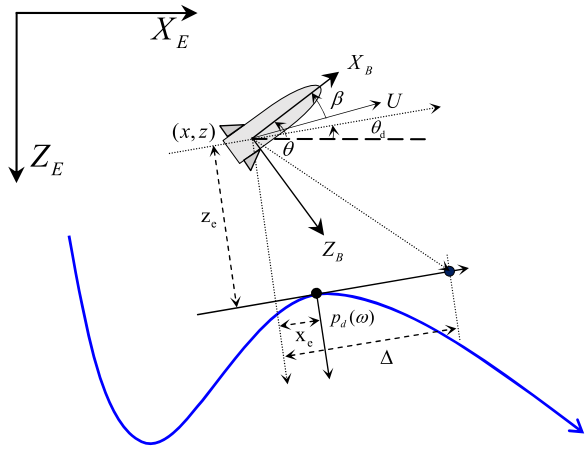

Fig. 1. Reference frames.

The rest of this paper is structured as follows. Section II states the problem formulation. Section III presents the design and analysis of a neurodynamics-based LOS path-following controller. Section IV provides simulation results for control performance illustrations. Section V concludes this paper.

II. Problem Formulation

A. Model of an AUV in the Vertical Plane

In this subsection, an AUV model in the vertical plane is introduced. The AUV performs missions in a 3-D plane and has a motion of six degrees of freedom. Generally, its motion in the vertical plane and that in the horizontal plane are usually decoupled and considered independently in the controller design [46], [47]. Specifically, the motion of the underactuated AUV in the vertical plane (X_E–Z_E) can be expressed by kinematic equations

$$\begin{cases} \dot{x} = u\cos\theta + w\sin\theta \\ \dot{z} = -u\sin\theta + w\cos\theta \\ \dot{\theta} = q \end{cases} \tag{1}$$

and kinetic equations

$$\begin{cases} m_u\dot{u} = f_u(t,u,w,q) + \tau_u + \tau_{du} \\ m_w\dot{w} = f_w(t,u,w,q) + \tau_{dw} \\ m_q\dot{q} = f_q(t,u,w,q) + \tau_q + \tau_{dq} \end{cases} \tag{2}$$

where x and z are the positions in the X_E–Z_E coordinate frame; u and w are the surge and heave speed in the X_B–Z_B coordinate frame, respectively; θ and q are the pitch angle and

angular rate, respectively; m_u, m_w, and m_q denote mass including hydrodynamic added mass; τ_{du}, τ_{dw}, and τ_{dq} denote the external environmental disturbance; τ_u and τ_q are control inputs; and $f_u(t,u,w,q)$, $f_w(t,u,w,q)$, and $f_q(t,u,w,q)$ are nonlinear functions related to hydrodynamic damping effects, which are totally unknown.

For the AUV, the linear and angular velocities are naturally bounded as

$$u_{\min} \le u \le u_{\max}, \quad w_{\min} \le w \le w_{\max}, \quad q_{\min} \le q \le q_{\max} \tag{3}$$

where $u_{\min}$, $u_{\max}$, $w_{\min}$, $w_{\max}$, $q_{\min}$, and $q_{\max}$ are lower and upper bounds, which are not necessary to be constants. Besides, the following constraints are imposed on the control inputs:

$$\tau_{\min}^u \le \tau_u \le \tau_{\max}^u, \quad \tau_{\min}^q \le \tau_q \le \tau_{\max}^q \tag{4}$$

where $\tau_{\min}^u$, $\tau_{\max}^u$, $\tau_{\min}^q$, and $\tau_{\max}^q$ are variable bounds on the force and moment.

B. Kinematic Path-Following Error

In this subsection, the path-following error dynamics is derived. At first, consider a parameterized path $p_d(\chi) = [x_d(\chi), z_d(\chi)] \in \Re^2$ expressed in the X_E–Z_E coordinate frame and define $\theta_d(\chi) = \arctan(-z_d'(\chi)/x_d'(\chi))$, where $\chi \in \Re$ is a parametric variable; $z_d'(\chi)$ and $x_d'(\chi)$ are the partial derivatives of $z_d(\chi)$ and $x_d(\chi)$, respectively.

Let $x_e \in \Re$ be an along-track error and $z_e \in \Re$ a cross-track error, which are expressed in the X_E–Z_E coordinate frame as

$$\begin{bmatrix} x_e \\ z_e \end{bmatrix} = \begin{bmatrix} \cos(\theta_d) & -\sin(\theta_d) \\ \sin(\theta_d) & \cos(\theta_d) \end{bmatrix} \begin{bmatrix} x - x_d(\chi) \\ z - z_d(\chi) \end{bmatrix}. \tag{5}$$

Differentiating x_e and z_e along (1) yields

$$\begin{cases} \dot{x}_e = u\cos(e_\theta) + w\sin(e_\theta) + \dot{\theta}_d z_e - u_d^* \dot{\chi} \\ \dot{z}_e = -u\sin(e_\theta) + w\cos(e_\theta) - \dot{\theta}_d x_e \\ \dot{\theta} = q \end{cases} \tag{6}$$

where $u_d^* = \sqrt{z_d'^2(\chi) + x_d'^2(\chi)}$ and $e_\theta = \theta - \theta_d$ is a path angle tracking error.

The design objective is to develop a control law τ_u and τ_q in (2) to stabilize the path-following errors x_e and z_e in (6) without violating the state constraint (3) and input constraint (4).

III. Design and Analysis

In this section, the design and analysis of a path-following controller is presented. The path-following control law is divided into three parts: an outer-loop guidance law designed at the kinematic level; an inner-loop control law designed at the kinetic level; and a neurodynamics-based reference governor.

A. Outer-Loop Guidance Law

In this subsection, an outer-loop guidance law is designed to stabilize the cross-track error z_e and the along-track error x_e in (6). To this end, the following notations are defined:

$$\begin{cases} l_u = u_o - u_c, \tilde{u} = \hat{u} - u, \hat{u}_e = \hat{u} - u_o \\ l_q = q_o - q_c, \tilde{q} = \hat{q} - q, \hat{q}_e = \hat{q} - q_o \\ \theta_e = \theta - \theta_c, \beta = \text{atan2}(w,u), \dot{\chi} = v_s - \chi_s \end{cases} \tag{7}$$

where u_c and q_c are commanded guidance signals, u_o and q_o are signals to be optimized, $\hat{u}$ and $\hat{q}$ are state estimations of u and q, $\tilde{u}$ and $\tilde{q}$ are estimation errors, $\hat{u}_e$ and $\hat{q}_e$ are estimated surge and pitch rate tracking errors, β is the angle of attack, v_s is a desired velocity for path updating, χ_s is a design variable, l_u is a mismatch term between the commanded surge velocity and optimal surge velocity, l_q is a mismatch term between the commanded pitch rate and optimal pitch rate, θ_c is a commanded pitch angle, and θ_e is the tracking error between the actual pitch angle and commanded pitch angle.

Using (7), the path-following equation in (6) is put into

$$\begin{cases} \dot{x}_e = l_u + \hat{u}_e - \tilde{u} + u_c - \bar{w} + \dot{\theta}_d z_e - u_d^*(v_s - \chi_s) \\ \dot{z}_e = -U\sin(\theta_c - \theta_d - \beta) - \dot{\theta}_d x_e + U\zeta \\ \dot{\theta}_e = l_q + \hat{q}_e - \tilde{q} + q_c - \dot{\theta}_c \end{cases} \tag{8}$$

where $U = \sqrt{u^2 + w^2} > 0$, $\zeta = \sin(\theta_c - \theta_d - \beta) - \sin(\theta - \theta_d - \beta)$, and $\bar{w} = 2u\sin^2(\frac{e_\theta}{2}) - w\sin(e_\theta)$.

Based on the LOS guidance principle, a commanded guidance law for (8) is proposed as follows:

$$\begin{cases} u_c = -k_x x_e + u_d^* v_s + \bar{w} - \hat{u}_e \\ q_c = -k_\theta \theta_e + \dot{\theta}_c - z_e U\zeta/\theta_e - \hat{q}_e \\ \theta_c = \arctan\left(\dfrac{z_e}{\Delta}\right) + \theta_d + \beta, \chi_s = -\mu x_e \end{cases} \tag{9}$$

where $\Delta \in \Re$ is a look-ahead distance; $k_x \in \Re$, $k_\theta \in \Re$, and $\mu \in \Re$ are control gains. Using (8) and (9), the dynamical path-following error equation in (8) can be expressed as

$$\begin{cases} \dot{x}_e = -k_x x_e + l_u - \tilde{u} + \dot{\theta}_d z_e - \mu u_d^* x_e \\ \dot{z}_e = -k_z z_e - \dot{\theta}_d x_e + U\zeta \\ \dot{\theta}_e = -k_\theta \theta_e + l_q - \tilde{q} - z_e U\zeta/\theta_e \end{cases} \tag{10}$$

where $k_z = U/\sqrt{\Delta^2 + z_e^2}$. Defining $E_1 = [x_e, z_e, \theta_e]^T$, $K = \text{diag}(k_x, k_z, k_\theta)$, $l_o = [l_u, 0, l_q]^T$, $l_d = [\tilde{u}, 0, \tilde{q}]^T$, and $\phi = [\dot{\theta}_d z_e - \mu u_d^* x_e, -\dot{\theta}_d x_e + U\zeta, -z_e U\zeta/\theta_e]^T$, it follows from (10) that

$$\dot{E}_1 = -KE_1 + l_o - l_d + \phi. \tag{11}$$

Lemma 1: The error dynamics in (11) with state vector being E_1 and the input vectors being l_o and l_d is input-to-state stable provided that $0 < U_{\min} \le U \le U_{\max}$.

Proof: Consider a Lyapunov function $V = \frac{1}{2}E_1^T E_1$. Taking the time derivative of V along (11) yields $\dot{V} = -E_1^T K E_1 + E_1^T l_o - E_1^T l_d \le -\lambda_{\min}(K)\|E_1\|^2 + \|E_1\|\|l_o\| + \|E_1\|\|l_d\|$. Since $\|E_1\| \ge (\|l_o\| + \|l_d\|)/(\lambda_{\min}(K)\bar{\theta})$ makes $\dot{V} \le -\lambda_{\min}(K)(1-\bar{\theta})\|E_1\|^2$, where $0 < \bar{\theta} < 1$, one can conclude that the subsystem (11) is input-to-state stable [48], and there exists a $\mathcal{KL}$ function $\alpha_1(\cdot)$ and class $\mathcal{K}_\infty$ functions $\gamma^{l_o}(\cdot)$ and $\gamma^{l_d}(\cdot)$ satisfying $\|E_1(t)\| \le \alpha_1(E_1(t_0), t - t_0) + \gamma^{l_o}(\|l_o\|) + \gamma^{l_d}(\|l_d\|)$, where $\gamma^{l_o}(s) = s/(\lambda_{\min}(K)\bar{\theta})$ and $\gamma^{l_d}(s) = s/(\lambda_{\min}(K)\bar{\theta})$.

In order to attenuate measurement noises, a filtered update law $\dot{\chi}_s = -k_\chi(\chi_s + \mu x_e)$ can be used to replace (9), where $k_\chi \in \Re$ is a positive constant. If multiple AUVs are considered, synchronized path following of AUVs can be achieved by modifying the update law for χ_s. ■

B. Inner-Loop Control Law

In the previous subsection, an outer-loop control law was developed at the kinematic level. In this subsection, an inner-loop control law will be designed at the kinetic level (2). As the hydrodynamic damping effects and external disturbance are unknown, their effect on control performance cannot be ignored. Here, an ESO is designed to estimate the unknown uncertainties in the AUV kinetics, at first. Next, a kinetic controller is derived based on an ESO.

The kinetic equations (2) in the surge and pitch directions can be expressed as

$$\dot{u} = \sigma_u + m_u^{-1}\tau_u, \quad \dot{q} = \sigma_q + m_q^{-1}\tau_q \tag{12}$$

where $\sigma_u = m_u^{-1} f_u(t,u,w,q) + m_u^{-1}\tau_{du}$ and $\sigma_q = m_q^{-1} f_r(t,u,w,q) + m_q^{-1}\tau_{dq}$. Both linear and nonlinear ESOs can be used to estimate σ_u and σ_q. In terms of accuracy, nonlinear ESOs can be more accurate than linear ones. However, linear ESOs outperform nonlinear ESOs in the presence of measurement noises.

Let $\hat{\sigma}_u$ and $\hat{\sigma}_q$ be the estimations of σ_u and σ_q, respectively, and an ESO is developed as

$$\begin{cases} \dot{\hat{u}} = -k_1^u\tilde{u} + \hat{\sigma}_u + m_u^{-1}\tau_u, \dot{\hat{\sigma}}_u = -k_2^u\tilde{u} \\ \dot{\hat{q}} = -k_1^q\tilde{q} + \hat{\sigma}_q + m_q^{-1}\tau_q, \dot{\hat{\sigma}}_q = -k_2^q\tilde{q} \end{cases} \tag{13}$$

where $k_1^u \in \Re$, $k_2^u \in \Re$, $k_1^q \in \Re$, and $k_2^q \in \Re$ are observer gains. Let $\tilde{\sigma}_u = \hat{\sigma}_u - \sigma_u$ and $\tilde{\sigma}_q = \hat{\sigma}_q - \sigma_q$. The error dynamics of the ESO can be obtained from (12) and (13) as

$$\dot{E}_2 = AE_2 - B\sigma \tag{14}$$

where $E_2 = [\tilde{u}, \tilde{\sigma}_u, \tilde{q}, \tilde{\sigma}_q]^T$, $\sigma = [\dot{\sigma}_u, \dot{\sigma}_q]^T$, and

$$A = \begin{bmatrix} -k_1^u & 1 & 0 & 0 \\ -k_2^u & 0 & 0 & 0 \\ 0 & 0 & -k_1^q & 1 \\ 0 & 0 & -k_2^q & 0 \end{bmatrix}, \quad B = \begin{bmatrix} 0 & 0 \\ 1 & 0 \\ 0 & 0 \\ 0 & 1 \end{bmatrix}. \tag{15}$$

Because A is a Hurwitz matrix, there exists a positive definite matrix P such that $A^T P + PA = -\varepsilon I_4$, where $\varepsilon \in \Re$ is a positive constant.

To analyze the stability of (14), the following usual assumptions are made.

Assumption 1: For $i = u, w, q$, the functions $f_i(t,u,w,q)$ satisfy $|f_i(\cdot)| + |\frac{\partial f_i(\cdot)}{\partial t}| + |\frac{\partial f_i(\cdot)}{\partial u}| + |\frac{\partial f_i(\cdot)}{\partial w}| + |\frac{\partial f_i(\cdot)}{\partial q}| \le c_0 + c_1|u|^k + c_2|w|^k + c_3|q|^k$, where c_0, c_1, c_2, and c_3 are positive constants and k is a positive integer.

Assumption 2: The disturbance τ_{di} and its derivative are bounded, i.e., $|\tau_{di}(t)| + |\dot{\tau}_{di}(t)| + |\tau_u| + |\tau_q| < \infty$.

Assumptions 1 and 2 are reasonable due to the limited internal and external energy to drive vehicles. The similar assumptions are made in [49].

Lemma 2: Under Assumptions 1 and 2, the ESO subsystem (14) with state vector being E_2 and the input vector being σ is input-to-state stable.

Proof: Consider a function $V = \frac{1}{2}E_2^T PE_2$, and its time derivative along (14) is given by $\dot{V} \le -\frac{\varepsilon}{2}\|E_2\|^2 + \|E_2\|\|PB\|\|\sigma\|$. As $\|E_2\| \ge 2\|PB\|\|\sigma\|/(\varepsilon\bar{\theta})$ renders $\dot{V} \le -\frac{\varepsilon}{2}(1-\bar{\theta})\|E_2\|^2$, it follows that the subsystem (14) is input-to-state stable. In what follows, there exists a $\mathcal{KL}$ function α_2 and a $\mathcal{K}_\infty$ function $\gamma^\sigma(\cdot)$ such that $\|E_2(t)\| \le \alpha_2(E_2(t_0), t-t_0) + \gamma^\sigma(\|\sigma\|)$, where $\gamma^\sigma(s) = 2\sqrt{\lambda_{\max}(P)/\lambda_{\min}(P)}\|PB\|s/(\varepsilon\bar{\theta})$. ■

The time derivatives of $\hat{u}_e$ and $\hat{q}_e$ from (13) can be expressed by

$$\begin{cases} \dot{\hat{u}}_e = -k_1^u\tilde{u} + \hat{\sigma}_u + m_u^{-1}\tau_u - \dot{u}_o \\ \dot{\hat{q}}_e = -k_1^q\tilde{q} + \hat{\sigma}_q + m_q^{-1}\tau_q - \dot{q}_o \end{cases}. \tag{16}$$

Using the estimated information of $\hat{\sigma}_u$ and $\hat{\sigma}_q$ from the ESO, an antidisturbance control law is proposed as

$$\tau_u = m_u(-k_u u_e - \hat{\sigma}_u), \quad \tau_q = m_q(-k_q q_e - \hat{\sigma}_q) \tag{17}$$

where $k_u \in \Re$ and $k_q \in \Re$ are positive constants. $u_e = u - u_o$ and $q_e = q - q_o$. From (17), the estimated tracking error dynamics of $\hat{u}_e$ and $\hat{q}_e$ can be expressed as

$$\begin{cases} \dot{\hat{u}}_e = -k_u\hat{u}_e - \varrho_u\tilde{u} - \dot{u}_o \\ \dot{\hat{q}}_e = -k_q\hat{q}_e - \varrho_q\tilde{q} - \dot{q}_o \end{cases} \tag{18}$$

where $\varrho_u = k_1^u - k_u$ and $\varrho_q = k_1^q - k_q$. The bandwidth of ESO (13) is designed larger than that of the kinetic control law (17) to satisfy $\varrho_u > 0$ and $\varrho_q > 0$. Letting $E_3 = [u_e, q_e]^T$, $\hat{E}_3 = [\hat{u}_e, \hat{q}_e]^T$, $K_c = \mathrm{diag}\{k_u, k_q\}$, $K_\varrho = \mathrm{diag}\{\varrho_u, \varrho_q\}$, $l_e = [\tilde{u}, \tilde{q}]^T$, and $l_b = [\dot{u}_o, \dot{q}_o]^T$, it follows that:

$$\dot{\hat{E}}_3 = -K_c\hat{E}_3 - K_\varrho l_e - l_b. \tag{19}$$

■

Lemma 3: The estimated tracking error dynamics (19) with the state vector being $\hat{E}_3$ and the input vectors being l_e and l_b is input-to-state stable.

Proof: Consider a Lyapunov function $V = \frac{1}{2}\hat{E}_3^T\hat{E}_3$, and its time derivative along (19) is given by $\dot{V} \le -\lambda_{\min}(K_c)\|\hat{E}_3\|^2 + \lambda_{\max}(K_\varrho)\|E_2\|\|\hat{E}_3\| + \|l_b\|\|\hat{E}_3\|$. Note that $\|\hat{E}_3\| \ge (\lambda_{\max}(K_\varrho)\|E_2\| + \|l_b\|)/(\lambda_{\min}(K_c)\bar{\theta})$ makes $\dot{V} \le -\lambda_{\min}(K_c)(1-\bar{\theta})\|\hat{E}_3\|^2$, and there exists a class $\mathcal{KL}$ function $\alpha_3(\cdot)$ and class $\mathcal{K}_\infty$ functions $\gamma^{E_2}(\cdot)$ and $\gamma^{l_b}(\cdot)$ such that $\|\hat{E}_3(t)\| \le \alpha_3(\|\hat{E}_3(t_0)\|, t-t_0) + \gamma^{E_2}(\|E_2\|) + \gamma^{l_b}(\|l_b\|)$, where $\gamma^{E_2}(s) = \lambda_{\max}(K_\varrho)s/(\lambda_{\min}(K_c)\bar{\theta})$ and $\gamma^{l_b}(s) = s/(\lambda_{\min}(K_c)\bar{\theta})$. ■

C. Neurodynamics-Based Reference Governor

In the previous subsection, an inner-loop controller was developed based on the prescribed signals of u_o and q_o. This section aims to present a neurodynamics-based reference governor for generating the optimal guidance signals. To satisfy the velocity constraints, the following constraints on the surge speed and pitch rate are enforced:

$$\underline{u} \le u_o \le \bar{u}, \underline{q} \le q_o \le \bar{q} \tag{20}$$

where $\underline{u} \in \Re$, $\bar{u} \in \Re$, $\underline{q} \in \Re$, and $\bar{q} \in \Re$ are designed to satisfy $u_{\min} < \underline{u}$, $\bar{u} < u_{\max}$, $q_{\min} < \underline{q}$, and $\bar{q} < q_{\max}$, respectively.

Using (4) and (17), it follows that $m_u(-k_u(u-u_o)-\hat{\sigma}_u) \le \tau^u_{\max}$, $m_u(k_u(u-u_o)+\hat{\sigma}_u) \le -\tau^u_{\min}$, $m_q(-k_q(q-q_o)-\hat{\sigma}_q) \le \tau^q_{\max}$, and $m_q(k_q(q-q_o)+\hat{\sigma}_q) \le -\tau^q_{\min}$, which can be further put into $u+\hat{\sigma}_u/k_u+\tau^u_{\min}/(m_u k_u) \le u_o \le u+\hat{\sigma}_u/k_u+\tau^u_{\max}/(m_u k_u), q+\hat{\sigma}_q/k_q+\tau^q_{\min}/(m_q k_q) \le q_o \le q+\hat{\sigma}_q/k_q+\tau^q_{\max}/(m_q k_q)$. As a result, the following constraints on surge speed and pitch rate are obtained:

$$\underline{\rho}_1 \le u_o \le \bar{\rho}_1, \quad \underline{\rho}_2 \le q_o \le \bar{\rho}_2 \tag{21}$$

where $\bar{\rho}_1 = \min\{\bar{u}, u+\hat{\sigma}_u/k_u+\tau^u_{\max}/(m_u k_u)\}$, $\underline{\rho}_1 = \max\{\underline{u}, u+\hat{\sigma}_u/k_u+\tau^u_{\min}/(m_u k_u)\}$, $\bar{\rho}_2 = \min\{\bar{q}, q+\hat{\sigma}_q/k_q+\tau^q_{\max}/(m_q k_q)\}$, and $\underline{\rho}_2 = \max\{\underline{q}, q+\hat{\sigma}_q/k_q+\tau^q_{\min}/(m_q k_q)\}$. Since the energy to drive AUVs is limited, the following instantaneous energy constraint is considered: $g(\rho) = m_u u_0^2/2 + m_q q_o^2/2 - E_{\max} \le 0$, where $E_{\max}$ is the maximal kinetic energy available in the AUV.

Let $\rho = [u_o, q_o]^T$. A cost function is defined for generating optimal reference signals as follows:

$$\begin{aligned} \min_{\rho} J(\rho) = {} & \frac{\lambda^u_1}{2}(u_o-u_c)^2 + \frac{\lambda^u_2}{2}(u_o-u)^2 \\ & + \frac{\lambda^q_1}{2}(q_o-q_c)^2 + \frac{\lambda^q_2}{2}(q_o-q)^2 \\ & \text{s.t. } \underline{\rho} \le \rho \le \bar{\rho}, g(\rho) \le 0 \end{aligned} \tag{22}$$

where $\underline{\rho} = [\underline{\rho}_1, \underline{\rho}_2]^T$, $\bar{\rho} = [\bar{\rho}_1, \bar{\rho}_2]^T$, and $\lambda^u_1 \in \Re$, $\lambda^u_2 \in \Re$, $\lambda^q_1 \in \Re$, and $\lambda^q_2 \in \Re$ are positive constants.

Problem (22) is a convex optimization problem. Let u^* and q^* be the optimal solution to the problem in (22). Then, the optimal control inputs can be obtained as $\tau_u = m_u[-k_u(u-u^*)-\hat{\sigma}_u]$, $\tau_q = m_q[-k_q(q-q^*)-\hat{\sigma}_q]$, which would not violate the input constraint (4).

Neurodynamic optimization is an efficient and powerful method for solving optimization problems [50], [51]. In order to solve the quadratically constrained optimization problem in (22), the following projection neural network is employed [51]:

$$\epsilon \frac{d}{dt}\begin{pmatrix}\rho \\ y\end{pmatrix} = \begin{pmatrix}\rho - P_r(\rho - \nabla J(\rho) - \nabla g(\rho) y) \\ -y + (y + g(\rho))^+\end{pmatrix} \tag{23}$$

where $(y)^+ = \max\{0, y\}$ and $P_r(\rho)$ is an activation function defined as $P_r(\rho_i) = \min_2\{\underline{\rho}_i, \rho_i, \bar{\rho}_i\}$, where ρ_i denotes the ith component of the vector ρ and $\min_2$ denotes the second smallest entry of a set.

It is proved in [51] that the projection neural network in (23) is exponentially convergent to its optimal solution. The convergence time is proportional to the time constant ϵ, and the optimal solution can be obtained in real time by choosing a small parameter ϵ. In implementations, the time scale of the projection neural network can be made faster than that of the control law (17). MPC methods employ multiple predictions for optimization [38], whereas the reference governor can be reviewed as an MPC controller with a prediction horizon one. As a result, the optimization burden of the reference governor is lighter than MPC methods.

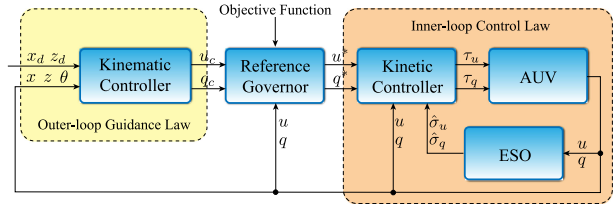

Fig. 2. Guidance and control architecture for vertical LOS path following.

D. Stability Analysis

Theorem 1: Under Assumptions 1 and 2, the cascade system formed by the kinematic control subsystem (11), the ESO subsystem (14), and the kinetic control subsystem (19) is input-to-state stable. Moreover, the tracking errors E_1 and E_3 are uniformly and ultimately bounded and can be reduced by selecting the control parameters.

Proof: Since subsystems (11), (14), and (19) are input-to-state stable, it follows from [52, Lemma C.4] that the cascade system is input-to-state stable. Because $\alpha_1(\cdot)$, $\alpha_2(\cdot)$, and $\alpha_3(\cdot)$ vanish as $t \to \infty$, $\|E_1(t)\|$ and $\|\hat{E}_3(t)\|$ are ultimately bounded by $\|E_1(t)\|_{t\to\infty} \le \gamma^{l_o} \circ \gamma^{\sigma}(\|\sigma\|) + \gamma^{l_o}(\|l_o\|) \le 2\sqrt{\lambda_{\max}(P)/\lambda_{\min}(P)}\|PB\| \, \|\sigma\|/(\lambda_{\min}(K)\varepsilon\bar{\theta}^2) + \|l_o\|/(\lambda_{\min}(K)\bar{\theta})$ and $\|\hat{E}_3(t)\|_{t\to\infty} \le \gamma^{E_2} \circ \gamma^{\sigma}(\|\sigma\|) + \gamma^{l_b}(\|l_b\|) \le 2\sqrt{\lambda_{\max}(P)/\lambda_{\min}(P)}(\lambda_{\max}(K_\varrho)\|PB\|\|\sigma\|)/(\lambda_{\min}(K_c)\varepsilon\bar{\theta}^2) + \|l_b\|/(\lambda_{\min}(K_c)\bar{\theta})$. Since $\|E_3(t)\| \le \|\hat{E}_3(t)\| + \|E_2(t)\|$ and $\|E_2(t)\|_{t\to\infty} \le 2\sqrt{\lambda_{\max}(P)/\lambda_{\min}(P)}\|PB\|\|\sigma\|/(\varepsilon\bar{\theta})$, it follows that $\|E_3(t)\|_{t\to\infty} \le (\lambda_{\max}(K_\varrho)/\lambda_{\min}(K_c) + \bar{\theta}) 2\sqrt{\lambda_{\max}(P)/\lambda_{\min}(P)}\|PB\|\|\sigma\|/(\varepsilon\bar{\theta}^2) + \|l_b\|/(\lambda_{\min}(K_c)\bar{\theta})$. From (3), there exists a constant σ^* such that $\|\sigma\| \le \sigma^*$. The exponential convergence property of the projection neural network means that J in (22) can be minimized. Hence, there exist positive constants l^*_u and l^*_q such that $|l_u| \le l^*_u$ and $|l_q| \le l^*_q$. Then, one has $\|l_o\| \le l^*_o$ with $l^*_o = \sqrt{(l^*_u)^2 + (l^*_q)^2}$. From (23), $\dot{q}_o$ and $\dot{u}_o$ are bounded due to the projection operator, implying that $\|l_b\| \le l^*_b$ with l^*_b being a positive constant. As a result, $\|E_1(t)\|_{t\to\infty} \le 2\sqrt{\lambda_{\max}(P)/\lambda_{\min}(P)}\|PB\|\sigma^*/(\lambda_{\min}(K)\varepsilon\bar{\theta}^2) + l^*_o/(\lambda_{\min}(K)\bar{\theta})$ and $\|E_3(t)\|_{t\to\infty} \le 2(\lambda_{\max}(K_\varrho)/\lambda_{\min}(K_c) + \bar{\theta})\sqrt{\lambda_{\max}(P)/\lambda_{\min}(P)}\|PB\| \sigma^*/(\varepsilon\bar{\theta}^2) + l^*_b/(\lambda_{\min}(K_c)\bar{\theta})$. ■

A guideline is provided for selecting parameters. k_x and k_θ determine the desired output responses, and a tradeoff should be made between response speed and stability margin. The observer gains can be selected as $[k^u_1, k^u_2]^T = [2\omega^u_o, (\omega^u_o)^2]^T$ and $[k^q_1, k^q_2]^T = [2\omega^q_o, (\omega^q_o)^2]^T$, where ω^u_o and ω^q_o are desired bandwidths. Accordingly, the kinetic control gains can be chosen as $\omega^u_o/10 \le k_u \le \omega^u_o/5$ and $\omega^q_o/10 \le k_q \le \omega^q_o/5$. The presented guidance and control architecture for vertical LOS path following of AUVs is illustrated in Fig. 2.

Remark 1: The proposed control method is applied to an AUV model of three degrees of freedom only, and an extension to an AUV model with six degrees of freedom is desirable.

Remark 2: The work in [38] aims to address the constrained kinetic control of a fully actuated AUV based on MPC, whereas

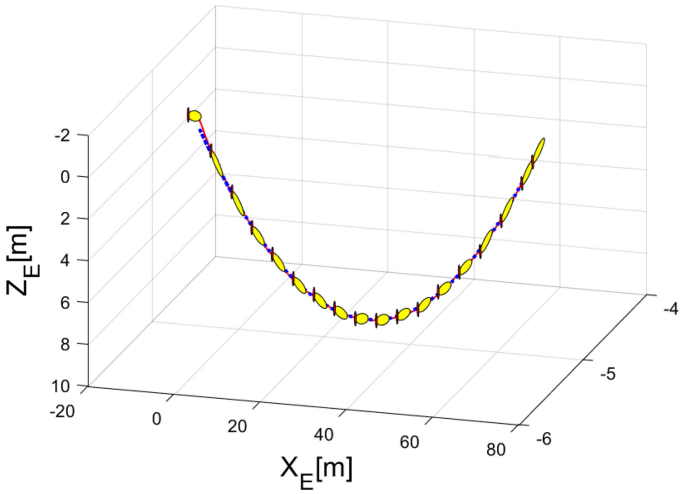

Fig. 3. Motion trajectory of the AUV.

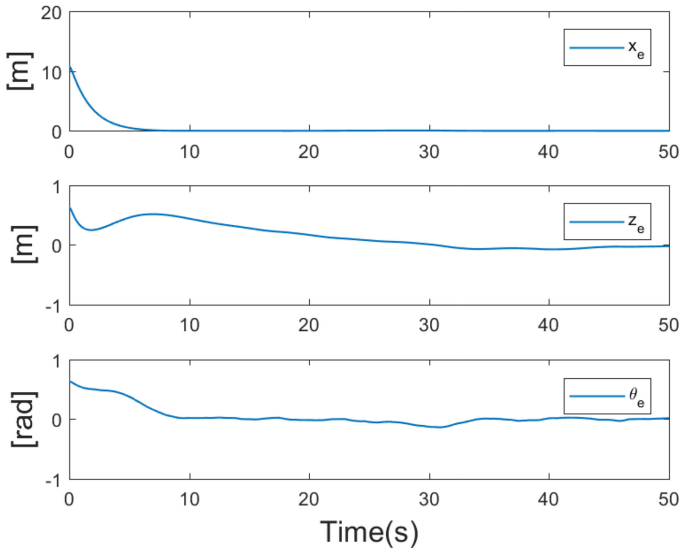

Fig. 4. Path-following errors x_e, z_e, and θ_e.

this paper addresses the constrained path following of an underactuated AUV without using MPC.

IV. Simulation Results

Consider an AUV with its model parameters given in [47]. In addition, time-varying disturbances modeled as first-order Gauss–Markov processes are introduced. For comparisons, some sudden changes on disturbances are added during 20–30 s. The AUV is set to track a trajectory parameterized by $x_d = \chi, z_d = -\chi^2/180 + \chi/3 + 4,$ and $\theta_d = \arctan(-\chi/90 + 1/3)$. For illustrations, the proposed method is compared with proportional-integral (PI) control and ESO-based control. The kinematic controllers for the three methods are all taken as (9). At the kinetic level, the PI control law is given by $\tau_u = -K_u^P(u-u_c) \quad -K_u^I\int_0^t(u-u_c)dt, \tau_q = -K_q^P(q-q_c) -K_q^I\int_0^t(q-q_c)dt$, and the ESO-based control law is given by $\tau_u = m_u[-k_u(u-u_c)-\hat{\sigma}_u], \tau_q = m_q[-k_q(q-q_c)-\hat{\sigma}_q]$, where K_u^P, K_u^I, K_q^P, and K_q^I are control parameters.

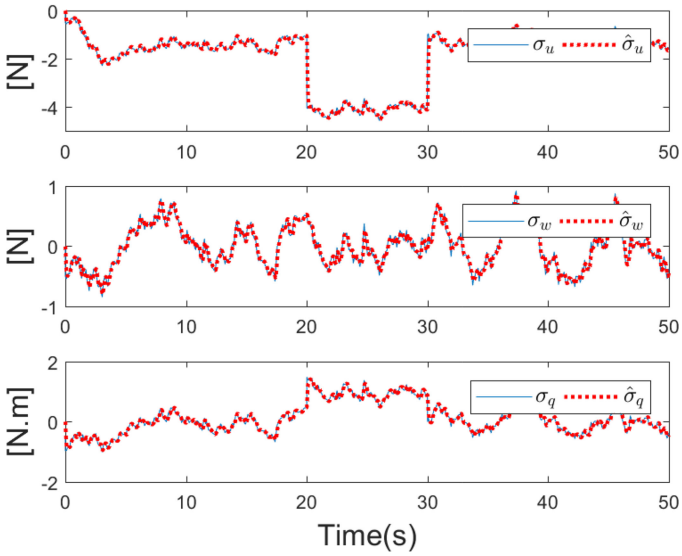

Fig. 5. Estimation performance by using the ESO.

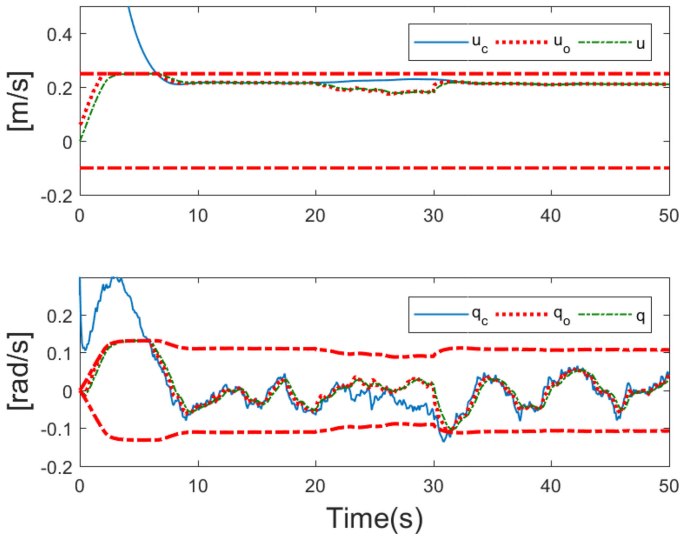

Fig. 6. Commanded signals, optimal reference signals, and actual signals of surge speed and pitch rate.

According to the parameter selection guideline, the control parameters are chosen as $k_x = 0.3$, $k_\theta = 0.4$, $\Delta = 2$, $k_\chi = 10$, $\mu = 0.5$, $k_u = 2$, $k_q = 4$, $k_1^u = 20$, $k_2^u = 100$, $k_1^q = 20$, $k_2^q = 100$, and $\epsilon = 0.0001$. The initial states of the AUV are set to $x(0) = -10\,\text{m}, z(0) = 0\,\text{m}, \theta(0) = 0\,\text{rad}, u(0) = 0\,\text{m/s}, w(0) = 0\,\text{m/s}$, and $q(0) = 0.1\,\text{rad/s}$. The lower and upper bounds for u and q are enforced as $\bar{u} = 0.25, \underline{u} = -0.1, \bar{q} = 0.42(u^2+u)$, and $\underline{q} = -\bar{q}$. Besides, the lower and upper bounds for τ_u and τ_q are taken as $\tau_{\max}^u = 4, \tau_{\min}^u = -1, \tau_{\max}^q = 4.2(u^2+u)$, and $\tau_{\min}^q = -\tau_{\max}^q$. The parameters for the ESO-based control law are taken as the same as the proposed controller. The parameters for the PI controller are selected as $K_u^P = m_u k_u$, $K_u^I = 1$, $K_q^P = m_q k_q$, and $K_q^I = 1$.

Simulation results are provided in Figs. 3–9. Specifically, Fig. 3 shows that the AUV is capable of tracking the given path even though perturbed by internal and external disturbances. Fig. 4 illustrates that the tracking errors x_e, z_e, and θ_e converge

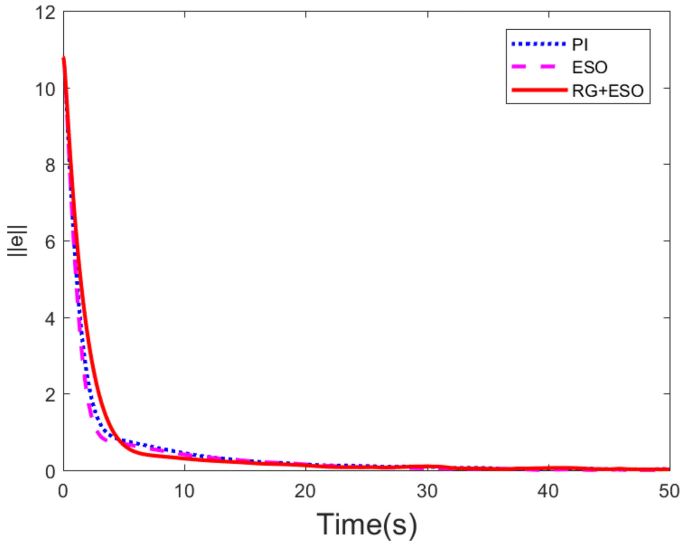

Fig. 7. Path-following error norms, where $e = [x_e, z_e, \theta_e]^T$.

to a small neighborhood of the origin. The total uncertainty σ and the output of the ESO are plotted in Fig. 5. It reveals that the total uncertainty in each direction can be accurately estimated by the developed ESO even though the sudden changes on disturbances occur during 20–30 s. Fig. 6 depicts the profiles of the commanded surge speed and pitch rate, the actual surge speed and pitch rate, and the optimal guidance signals of surge speed and pitch rate. During the transient phase, the commanded surge speed and pitch rate violate the state constraints; the reference governor is able to balance the commanded signals and the actual signals of surge speed and pitch rate and prescribes optimal guidance signals. During 20–30 s, although the commanded surge speed and pitch rate are within the state constraints, the input constraints are violated due to the sudden disturbances. The reference governor generates modified guidance signals within the input constraints. Fig. 7 depicts the norms of path-following errors using the PI control method, the ESO-based control method, and the proposed method. As expected, the PI control method and the ESO-based control method achieve better performance during the transient phase because the constraints are not enforced for PI control and ESO-based control. Besides, the ESO-based control performs better than the PI control due to the capability to estimate and reject the internal and external disturbances actively. During the steady phase, the tracking performances of the three methods are almost the same. Figs. 8 and 9 depict the control inputs of the three methods in surge direction and in pitch direction, respectively. Both the PI control and ESO-based control violate the input constraints during the transient and steady phases when perturbed by large disturbances. In contrast, the proposed method is capable of computing optimal guidance signals without violating the input constraints in both transient and steady phases. In implementations, the complexity of the proposed method is higher than those of the PI control and ESO-based control. If the projection neural network is implemented in parallel to the path-following controller, the complexity of the three methods will be similar.

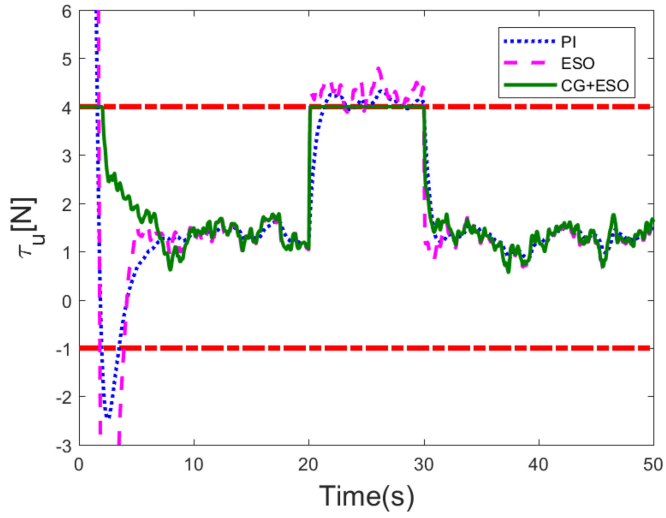

Fig. 8. Control inputs in surge direction.

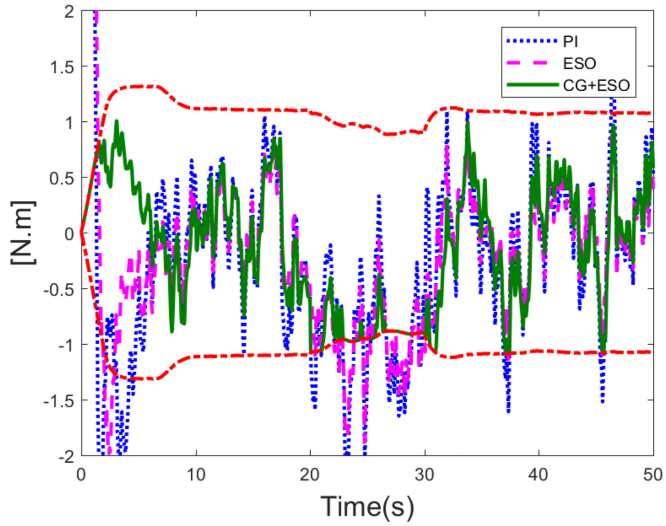

Fig. 9. Control inputs in pitch direction.

V. Conclusion

This paper considered the path-following control of underactuated AUVs subject to state and input constraints, as well as internal and external disturbances. The overall path-following control law included an outer-loop guidance law, an inner-loop kinetic control law, and a reference governor. Specifically, the outer-loop guidance law was to derive the desired surge speed and pitch rate based on an LOS guidance scheme and a backstepping technique. The inner-loop kinetic control law was devised based on an ESO such that the total uncertainty in vehicle kinetics could be estimated and rejected. The reference governor was used for generating the optimal reference signals within the state and input constraints, and a projection neural network was used to solve the optimization problem. The simulation results substantiated the efficacy of the proposed path-following controller for underactuated AUVs in the presence of constraints and disturbances.

Due to the limited computing power and communication bandwidth of AUVs, the quantization of transmission signal

and data packet dropout may occur, which affect the control performance. Therefore, it is desirable to consider these issues in future works [53]–[55]. Besides, approximators are powerful tools to deal with nonlinear systems with uncertainties [56]–[59], and it is desirable to investigate the path-following control of AUVs by using fuzzy logic systems or neural networks.

REFERENCES

[1] K. Do, J. Pan, and Z. Jiang, "Robust and adaptive path following for underactuated autonomous underwater vehicles," *Ocean Eng.*, vol. 31, no. 16, pp. 1967–1997, Nov. 2004.

[2] L. Lapierre and D. Soetanto, "Nonlinear path-following control of an AUV," *Ocean Eng.*, vol. 34, nos. 11/12, pp. 1734–1744, Aug. 2007.

[3] L. Lapierre and B. Jouvencel, "Robust nonlinear path-following control of an AUV," *IEEE J. Ocean. Eng.*, vol. 33, no. 2, pp. 89–102, Apr. 2008.

[4] A. P. Aguiar and J. P. Hespanha, "Trajectory-tracking and path-following of underactuated autonomous vehicles with parametric modeling uncertainty," *IEEE Trans. Autom. Control*, vol. 52, no. 8, pp. 1362–1379, Aug. 2007.

[5] R. Cui, L. Chen, C. Yang, and M. Chen, "Extended state observer-based integral sliding mode control for an underwater robot with unknown disturbances and uncertain nonlinearities," *IEEE Trans. Ind. Electron.*, vol. 68, no. 4, pp. 6785–6795, Aug. 2017.

[6] Y. Shi, C. Shen, H. Fang, and H. Li, "Advanced control in marine mechatronic systems: A survey," *IEEE/ASME Trans. Mechatronics*, vol. 22, no. 3, pp. 1121–1131, Jun. 2017.

[7] R. Cui, X. Zhang, and D. Cui, "Adaptive sliding-mode attitude control for autonomous underwater vehicles with input nonlinearities," *Ocean. Eng.*, vol. 123, pp. 45–54, Sep. 2016.

[8] Z. Chu, X. Xiang, D. Zhu, C. Luo, and D. Xie, "Adaptive fuzzy sliding mode diving control for autonomous underwater vehicle with input constraint," *Int. J. Fuzzy Syst.*, vol. 20, no. 5, pp. 1460–1469, Sep. 2018.

[9] Y.-L. Wang and Q.-L. Han, "Network-based fault detection filter and controller coordinated design for unmanned surface vehicles in network environments," *IEEE Trans. Ind. Inform.*, vol. 12, no. 5, pp. 1753–1765, Oct. 2016.

[10] Y.-L. Wang, Q.-L. Han, M.-R. Fei, and C. Peng, "Network-based T-S fuzzy dynamic positioning controller design for unmanned marine vehicles," *IEEE Trans. Cybern.*, vol. 48, no. 9, pp. 2750–2763, Sep. 2018.

[11] S. Yin, H. Yang, and O. Kaynak, "Coordination task triggered formation control algorithm for multiple marine vessels," *IEEE Trans. Ind. Electron.*, vol. 64, no. 6, pp. 4984–4993, May 2017.

[12] T. I. Fossen and K. Y. Pettersen, "On uniform semiglobal exponential stability (USGES) of proportional line-of-sight guidance laws," *Automatica*, vol. 50, no. 11, pp. 2912–2917, Nov. 2014.

[13] A. M. Lekkas and T. I. Fossen, "Integral LOS path following for curved paths based on a monotone cubic Hermite spline parametrization," *IEEE Trans. Control Syst. Technol.*, vol. 22, no. 6, pp. 2287–2301, Nov. 2014.

[14] T. I. Fossen, K. Y. Pettersen, and R. Galeazzi, "Line-of-sight path following for Dubins paths with adaptive sideslip compensation of drift forces," *IEEE Trans. Control Syst. Technol.*, vol. 23, no. 2, pp. 820–827, Mar. 2015.

[15] X. Xiang, C. Yu, L. Lapierre, J. Zhang, and Q. Zhang, "Survey on fuzzy-logic-based guidance and control of marine surface vehicles and underwater vehicles," *Int. J. Fuzzy Syst.*, vol. 20, no. 2, pp. 572–586, Feb. 2018.

[16] W. Caharija *et al.*, "Integral line-of-sight guidance and control of underactuated marine vehicles: Theory, simulations, and experiments," *IEEE Trans. Control Syst. Technol.*, vol. 24, no. 5, pp. 1623–1642, Sep. 2016.

[17] X. Xiang, L. Lapierre, and B. Jouvencel, "Smooth transition of AUV motion control: From fully-actuated to under-actuated configuration," *Robotics Auton. Syst.*, vol. 67, pp. 14–22, May 2015.

[18] R. Cui, S. S. Ge, B. V. E. How, and Y. S. Choo, "Leader–follower formation control of underactuated autonomous underwater vehicles," *Ocean. Eng.*, vol. 37, nos. 17/18, pp. 1491–1502, Dec. 2010.

[19] Z. Peng, D. Wang, Z. Chen, X. Hu, and W. Lan, "Adaptive dynamic surface control for formations of autonomous surface vehicles with uncertain dynamics," *IEEE Trans. Control Syst. Technol.*, vol. 21, no. 2, pp. 513–520, Mar. 2013.

[20] Z. Peng, D. Wang, Y. Shi, H. Wang, and W. Wang, "Containment control of networked autonomous underwater vehicles with model uncertainty and ocean disturbances guided by multiple leaders," *Inf. Sci.*, vol. 316, no. 12, pp. 163–179, Sep. 2015.

[21] Y.-L. Wang and Q.-L. Han, "Network-based modelling and dynamic output feedback control for unmanned marine vehicles in network environments," *Automatica*, vol. 91, pp. 43–53, May 2018.

[22] Z. Peng, J. Wang, and D. Wang, "Distributed containment maneuvering of multiple marine vessels via neurodynamics-based output feedback," *IEEE Trans. Ind. Electron.*, vol. 64, no. 5, pp. 3831–3839, May 2017.

[23] Z. Zheng, Y. Huang, L. Xie, and B. Zhu, "Adaptive trajectory tracking control of a fully actuated surface vessel with asymmetrically constrained input and output," *IEEE Trans. Control Syst. Technol.*, vol. 26, no. 5, pp. 1851–1859, Sep. 2018.

[24] L. Liu, D. Wang, Z. Peng, C. L. P. Chen, and T. Li, "Bounded neural network control for target tracking of underactuated autonomous surface vehicles in the presence of uncertain target dynamics," *IEEE Trans. Neural Netw. Learn. Syst.*, to be published, doi: 10.1109/TNNLS.2018.2868978.

[25] X. Ge and Q.-L. Han, "Distributed formation control of networked multi-agent systems using a dynamic event-triggered communication mechanism," *IEEE Trans. Ind. Electron.*, vol. 64, no. 10, pp. 8118–8127, Oct. 2017.

[26] X. Ge, Q.-L. Han, and X.-M. Zhang, "Achieving cluster formation of multiagent systems under aperiodic sampling and communication delays," *IEEE Trans. Ind. Electron.*, vol. 65, no. 4, pp. 3417–3426, Apr. 2018.

[27] L. Liu, D. Wang, Z. Peng, and H. Wang, "Predictor-based LOS guidance law for path following of underactuated marine surface vehicles with sideslip compensation," *Ocean. Eng.*, vol. 124, pp. 340–348, Sep. 2016.

[28] L. Liu, D. Wang, and Z. Peng, "ESO-based line-of-sight guidance law for path following of underactuated marine surface vehicles with exact sideslip compensation," *IEEE J. Ocean. Eng.*, vol. 42, no. 2, pp. 477–487, Apr. 2017.

[29] L. Liu, D. Wang, Z. Peng, and T. Li, "Modular adaptive control for LOS-based cooperative path maneuvering of multiple underactuated autonomous surface vehicles," *IEEE Trans. Syst., Man, Cybern.: Syst.*, vol. 47, no. 7, pp. 1613–1624, Jul. 2017.

[30] T. Wang, H. Gao, and J. Qiu, "A combined adaptive neural network and nonlinear model predictive control for multirate networked industrial process control," *IEEE Trans. Neural Netw. Learn. Syst.*, vol. 27, no. 2, pp. 416–425, Feb. 2016.

[31] T. Wang, J. Qiu, S. Yin, H. Gao, J. Fan, and T. Chai, "Performance-based adaptive fuzzy tracking control for networked industrial processes," *IEEE Trans. Cybern.*, vol. 46, no. 8, pp. 1760–1770, Aug. 2016.

[32] Z. Peng, J. Wang, and D. Wang, "Distributed maneuvering of autonomous surface vehicles based on neurodynamic optimization and fuzzy approximation," *IEEE Trans. Control Syst. Technol.*, vol. 26, no. 3, pp. 1083–1090, May 2018.

[33] T. Gao, S. Yin, H. Gao, X. Yang, J. Qiu, and O. Kaynak, "A locally weighted project regression approach-aided nonlinear constrained tracking control," *IEEE Trans. Neural Netw. Learn. Syst.*, vol. 29, no. 12, pp. 5870–5879, Dec. 2018, doi: 10.1109/TNNLS.2018.2808700.

[34] C. Shen, Y. Shi, and B. Buckham, "Trajectory tracking control of an autonomous underwater vehicle using Lyapunov-based model predictive control," *IEEE Trans. Ind. Electron.*, vol. 65, no. 7, pp. 5796–5805, Dec. 2017.

[35] C. Shen, Y. Shi, and B. Buckham, "Path-following control of an AUV: A multiobjective model predictive control approach," *IEEE Trans. Control Syst. Technol.*, to be published, doi: 10.1109/TCST.2018.2789440.

[36] Z. Chu, D. Zhu, S. X. Yang, and G. E. Jan, "Adaptive sliding mode control for depth trajectory tracking of remotely operated vehicle with thruster nonlinearity," *J. Navigat.*, vol. 70, no. 1, pp. 149–164, Jul. 2017.

[37] H. Li, P. Xie, and W. Yan, "Receding horizon formation tracking control of constrained underactuated autonomous underwater vehicles," *IEEE Trans. Ind. Electron.*, vol. 64, no. 6, pp. 5004 –5013, Jun. 2017.

[38] Z. Peng, J. Wang, and J. Wang, "Constrained control of autonomous underwater vehicles based on command optimization and disturbance estimation," *IEEE Trans. Ind. Electron.*, to be published, doi: 10.1109/TIE.2018.2856180.

[39] Z. Yan and J. Wang, "Model predictive control for tracking of underactuated vessels based on recurrent neural networks," *IEEE J. Ocean. Eng.*, vol. 37, no. 4, pp. 717–726, Oct. 2012.

[40] S.-R. Oh and J. Sun, "Path following of underactuated marine surface vessels using line-of-sight based model predictive control," *Ocean. Eng.*, vol. 37, nos. 2/3, pp. 289–295, Feb. 2010.

[41] M. Chen, S. S. Ge, B. V. E. How, and Y. S. Choo, "Robust adaptive position mooring control for marine vessels," *IEEE Trans. Control Syst. Technol.*, vol. 21, no. 2, pp. 395–409, Mar. 2013.

[42] B. J. Guerreiro, C. Silvestre, R. Cunha, and A. Pascoal, "Trajectory tracking nonlinear model predictive control for autonomous surface craft," *IEEE Trans. Control Syst. Technol.*, vol. 22, no. 6, pp. 2160–2175, Nov. 2014.
[43] D. Chwa, "Global tracking control of underactuated ships with input and velocity constraints using dynamic surface control method," *IEEE Trans. Control Syst. Technol.*, vol. 19, no. 6, pp. 1357–1370, Nov. 2011.
[44] Z. Zheng and L. Sun, "Path following control for marine surface vessel with uncertainties and input saturation," *Neurocomputing*, vol. 177, pp. 158–167, Feb. 2016.
[45] H. Li and W. Yan, "Model predictive stabilization of constrained underactuated autonomous underwater vehicles with guaranteed feasibility and stability," *IEEE/ASME Trans. Mechatronics*, vol. 22, no. 3, pp. 1185–1194, Jun. 2017.
[46] C. Silvestre, R. Cunha, N. Paulino, and A. Pascoal, "A bottom-following preview controller for autonomous underwater vehicles," *IEEE Trans. Control Syst. Technol.*, vol. 17, no. 2, pp. 257–266, Mar. 2009.
[47] A. Adhami-Mirhosseini, M. J. Yazdanpanah, and A. P. Aguiar, "Automatic bottom-following for underwater robotic vehicles," *Automatica*, vol. 50, no. 8, pp. 2155–2162, Aug. 2014.
[48] H. K. Khalil, *Nonlinear Control*. New York, NY, USA: Pearson Education, 2015.
[49] B.-Z. Guo and Z.-L. Zhao, "On the convergence of an extended state observer for nonlinear systems with uncertainty," *Syst. Control Lett.*, vol. 60, no. 6, pp. 420–430, Jun. 2011.
[50] Y. Xia and J. Wang, "A recurrent neural network for nonlinear convex optimization subject to nonlinear inequality constraints," *IEEE Trans. Circuits Syst. I, Reg. Papers*, vol. 51, no. 7, pp. 1385–1394, Jul. 2004.
[51] Y. Xia, "An extended projection neural network for constrained optimization," *Neural Comput.*, vol. 16, no. 4, pp. 863–883, Apr. 2004.
[52] M. Krstic, P. V. Kokotovic, and I. Kanellakopoulos, *Nonlinear and Adaptive Control Design*. New York, NY, USA: Wiley, 1995.
[53] X.-H. Chang, Z.-M. Li, and J. H. Park, "Fuzzy generalized H_2 filtering for nonlinear discrete-time systems with measurement quantization," *IEEE Trans. Syst., Man, Cybern.: Syst.*, vol. 48, no. 12, pp. 2419–2430, Dec. 2018.
[54] X.-H. Chang, Q. Liu, Y.-M. Wang, and J. Xiong, "Fuzzy peak-to-peak filtering for networked nonlinear systems with multipath data packet dropouts," *IEEE Trans. Fuzzy Syst.*, to be published, doi: 10.1109/TFUZZ.2018.2859903.
[55] X.-H. Chang, J. Xiong, Z.-M. Li, and J. H. Park, "Quantized static output feedback control for discrete-time systems," *IEEE Trans. Ind. Inform.*, vol. 14, no. 8, pp. 3426–3435, Aug. 2018.
[56] Y. Wang, H. R. Karimi, H. Shen, Z. Fang, and M. Liu, "Fuzzy-model-based sliding mode control of nonlinear descriptor systems," *IEEE Trans. Cybern.*, to be published, doi: 10.1109/TCYB.2018.2842920.
[57] Y. Wang, H. R. Karimi, H.-K. Lam, and H. Shen, "An improved result on exponential stabilization of sampled-data fuzzy systems," *IEEE Trans. Fuzzy Syst.*, vol. 26, no. 6, pp. 3875–3883, Dec. 2018.
[58] Y. Zhang, D. Wang, and Z. Peng, "Consensus maneuvering for a class of nonlinear multivehicle system in strict-feedback form," *IEEE Trans. Cybern.*, to be published, doi: 10.1109/TCYB.2018.2822258.
[59] Y. Wang, H. Shen, H. R. Karimi, and D. Duan, "Dissipativity-based fuzzy integral sliding mode control of continuous-time T-S fuzzy systems," *IEEE Trans. Fuzzy Syst.*, vol. 26, no. 3, pp. 1164–1176, Jun. 2018.

Zhouhua Peng (M'13) received the B.E. degree in electrical engineering and automation, the M.E. degree in power electronics and power drives, and the Ph.D. degree in control theory and control engineering from Dalian Maritime University, Dalian, China, in 2005, 2008, and 2011, respectively.

He is a Professor with the School of Marine Electrical Engineering, Dalian Maritime University. From 2014 to 2018, he was a Postdoctoral Researcher with the School of Control Science and Engineering, Dalian University of Technology, Dalian. From 2016 to 2018, he was a Hong Kong Scholar with the Department of Computer Science, City University of Hong Kong, Hong Kong. His research interests include formation control, intelligent control, antidisturbance control, and neurodynamic optimization methods with an emphasis on unmanned marine vehicles.

Jun Wang (F'07) received the B.S. degree in electrical engineering and the M.S. degree in systems engineering from the Dalian University of Technology, Dalian, China, in 1982 and 1985, respectively, and the Ph.D. degree in systems engineering from Case Western Reserve University, Cleveland, OH, USA, in 1991.

He is a Chair Professor with the Department of Computer Science, City University of Hong Kong, Kowloon, Hong Kong. Prior to this position, he held various academic positions with the Dalian University of Technology, Case Western Reserve University, the University of North Dakota, Grand Forks, ND, USA, and the Chinese University of Hong Kong, Shatin, Hong Kong. He also held various Part-Time Visiting Positions with the U.S. Air Force Armstrong Laboratory, the Rikagaku Kenkyusho Institute of Physical and Chemical Research Brain Science Institute, the Huazhong University of Science and Technology, the Dalian University of Technology, and Shanghai Jiao Tong University as a Changjiang Chair Professor.

Dr. Wang is the Editor-in-Chief of the IEEE TRANSACTIONS ON CYBERNETICS. He is a Fellow of the International Association for Pattern Recognition. He is a recipient of the IEEE TRANSACTIONS ON NEURAL NETWORKS Outstanding Paper Award, the Asia Pacific Neural Network Assembly Outstanding Achievement Award, and the Neural Networks Pioneer Award from the IEEE Computational Intelligence Society.

Qing-Long Han (F'19) received the B.S. degree in mathematics from Shandong Normal University, Jinan, China, in 1983, and the M.S. and Ph.D. degrees in control engineering and electrical engineering from the East China University of Science and Technology, Shanghai, China, in 1992 and 1997, respectively.

From 1997 to 1998, he was a Postdoctoral Researcher Fellow with the Laboratoire d'Automatique et d'Informatique Industielle (currently, Laboratoire d'Informatique et d'Automatique pour les Systémes), École Supérieure d'Ing'enieurs de Poitiers (currently, École Nationale Supérieure d'Ingénieurs de Poitiers), Université de Poitiers, France. From 1999 to 2001, he was a Research Assistant Professor with the Department of Mechanical and Industrial Engineering, Southern Illinois University, Edwardsville, IL, USA. From 2001 to 2014, he was Laureate Professor, an Associate Dean (Research and Innovation) with the Higher Education Division, and the Founding Director of the Centre for Intelligent and Networked Systems, Central Queensland University, Australia. From 2014 to 2016, he was the Deputy Dean (Research), with the Griffith Sciences, and a Professor with the Griffith School of Engineering, Griffith University, Australia. In 2016, he joined the Swinburne University of Technology, Melbourne, VIC, Australia, where he is currently a Pro Vice-Chancellor (Research Quality) and a Distinguished Professor. In 2010, he was appointed as a Chang Jiang (Yangtze River) Scholar Chair Professor by the Ministry of Education, China. His research interests include networked control systems, neural networks, time-delay systems, multiagent systems, and complex dynamical systems.